Bending Moment–Shear Force Interaction Domains for Prestressed Concrete Beams

Antonino Recupero[1]; Antonino D'Aveni[2]; and Aurelio Ghersi[3]

Abstract: The performance of a prestressed concrete beam, subjected to bending moment M together with shear force V, has been the object of many studies and is an important aspect to take into account in the design. Some models, proposed by researchers and international codes, evaluate the shear strength of prestressed beams by modifying the truss model by Morsch, so as to account for the different slope of stress fields in the web due to the prestressing action. More recent approaches add a strut-and-tie model to the traditional truss model. This paper generalizes a model that was previously proposed for box and I-shaped reinforced concrete cross sections of structural elements. The model, that now includes the effect of prestressing tendons, considers variable-depth stress fields applied to the cross section, subdivided into layers, and allows evaluation of normalized m–v design domains depending both on the web and flange reinforcement and on the slope of the prestressing steel tendons. The reliability of the method has been validated by comparing its numerical results to the strength provided by tests on reinforced concrete beams and on thin-webbed prestressed concrete beams, referred to in the literature. Finally, it has been used in the design of a pretensioned bridge beam to evaluate the additional reinforcement necessary in the flanges, as a function of the reinforcement provided to the web.

DOI: 10.1061/(ASCE)0733-9445(2005)131:9(1413)

CE Database subject headings: Concrete beams; Concrete, prestressed; Design; Models; Trusses.

Introduction

The large majority of codes propose different models for reinforced concrete structures and for prestressed elements (ACI Committee 318 1983; EC2 1996). In the case of reinforced concrete elements, the shear strength in the presence of axial force has been discussed by many authors, both referring to rectangular cross sections (Mattock 1969; Haddadin et al. 1971 Puleri et al. 1991; Fanti and Mancini 1995 Puleri and Russo 1997; Mancini and Recupero 2000; ;) and to T- or I-shaped cross sections (Recupero et al. 2003). Some of them proposed design formulations based on experimental results. Other researchers, starting from the stress fields approach by Bach et al. (1978), tried to obtain a more general model able to account for the simultaneous presence of different internal actions.

Different models have been proposed to evaluate shear-prestressing interaction (Schlaich et al. 1987; CEB-FIP 1993; Fanti and Mancini 1994; Fanti et al. 1995; Collins et al. 1996), once again obtaining design formulations by experimental results, or accounting for the prestressing tendons by adding a strut-and-tie model to the traditional truss model by Ritter and Morsch.

The analytical model here proposed is the generalization of a previously proposed model for the the axial force-bending moment-shear force (N–M–V) interaction, based on the stress fields approach, which now includes the effect of prestressing tendons, thus providing a unified approach for reinforced concrete and prestressed concrete elements. The reliability of the model has been validated by comparing its numerical results both to experimental results already analyzed for reinforced concrete beams and to the strength values obtained by means of failure tests performed on thin-webbed prestressed concrete beams, reported by Tan and Ng (1998). Finally, it has been used in the design of a pretensioned bridge beam, so as to show how it allows the evaluation of the additional reinforcement necessary in top and bottom flanges, in function of the longitudinal reinforcement provided to the web.

Analytical Model

The actual distribution of axial and shear stress in a beam, close to collapse, cannot be easily foreseen, because of the strong correlation between flexural and shear failure. Nevertheless, the physical evidence given by deformations and cracks suggests the use of a simplified layered model, in which the flanges and the outmost portion of the web resist only to axial stresses, while the central portion of the web is subjected also to shear stresses (Figs. 1 and 2). The ultimate resistance of a prestressed beam may thus be evaluated using a five-layer model, in which concrete and steel contributions are evaluated assuming that:

- The concrete flanges and the top and bottom portions of the web (having z_1 and z_2 depth, respectively) are subjected to

[1]Research Assistant, Dept. di Costruzioni e Tecnologie Avanzate, Univ. of Messina, Via Salita Sperone 31, 98166, Messina, Italy. E-mail: ninocosimo@tiscalinet.it

[2]Associate Professor, Dept. di Ingegneria Civile ed Ambientale, Univ. of Catania, Viale Andrea Doria 6, 95100, Catania, Italy. E-mail: adaveni@tiscalinet.it

[3]Professor, Dept. di Ingegneria Civile ed Ambientale, Univ. of Catania, Viale Andrea Doria 6, 95100, Catania, Italy (corresponding author). E-mail: aghersi@dica.unict.it

Note. Associate Editor: Dat Duthinh. Discussion open until February 1, 2006. Separate discussions must be submitted for individual papers. To extend the closing date by one month, a written request must be filed with the ASCE Managing Editor. The manuscript for this paper was submitted for review and possible publication on September 26, 2003; approved on November 1, 2004. This paper is part of the ***Journal of Structural Engineering***, Vol. 131, No. 9, September 1, 2005. ©ASCE, ISSN 0733-9445/2005/9-1413–1421/$25.00.

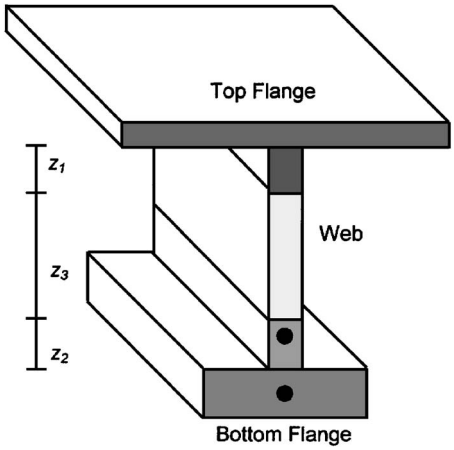

Fig. 1. Layered model of the structural element

uniform compressive stress fields, acting along the longitudinal direction (no tensile contribution of concrete at collapse is considered);

- The central portion of the web (having z_3 depth) is subjected to a uniform compressive stress field, acting with an angle of ϑ degrees to the longitudinal direction; this angle may vary during the loading process, because of the actions transmitted along the shear cracks; and
- The longitudinal reinforcements of the beam (located in the flanges and in the web) and the transverse reinforcements in the web give rise to stress fields, which are assumed to be uniformly distributed.

Consequently, the axial stresses σ_{ft}, σ_{fb}, σ_{w1}, σ_{w2} in the flanges and in the outermost portions of the web account for the contribution of the compressed concrete and of the longitudinal reinforcements. The axial and shear stresses σ_{w3}, τ in the central portion of the web are equivalent to the stress fields of the inclined strut and of the web transverse and longitudinal reinforcements.

The failure of the structural element may occur either by concrete crushing or by reinforcements yielding. Using the design values given by CEB-FIP (1993) for steel yielding f_{yd} and for concrete compression strength f_{cd1} and f_{cd2}, the following conditions are obtained:

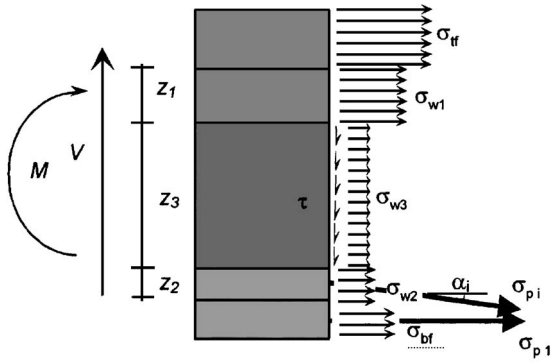

Fig. 2. Internal actions, prestressing forces, and stress distribution in the layers

- In the top and bottom flange layers:

$$-(f_{cd1}+\rho_{ft}f_{yd}) \leq \sigma_{ft} \leq \rho_{ft}f_{yd} \tag{1a}$$

$$-(f_{cd1}+\rho_{fb}f_{yd}) \leq \sigma_{fb} \leq \rho_{fb}f_{yd} \tag{1b}$$

- In the outermost web layers:

$$-(f_{cd1}+\rho_{wl}f_{yd}) \leq \sigma_{w1} \leq \rho_{wl}f_{yd} \tag{2a}$$

$$-(f_{cd1}+\rho_{wl}f_{yd}) \leq \sigma_{w2} \leq \rho_{wl}f_{yd} \tag{2b}$$

- In the central web layer:

$$-(\sigma_{w3}+\rho_{wl}f_{yd})\tan\vartheta \leq \tau \leq (-\sigma_{w3}+\rho_{wl}f_{yd})\tan\vartheta \tag{3a}$$

$$\tau \leq \rho_{wl}f_{yd}\cot\vartheta \tag{3b}$$

$$\tau \leq f_{cd2}\sin\vartheta\cos\vartheta \tag{3c}$$

Furthermore, each prestressing tendon is subjected to an axial force, acting with an angle of α degrees to the longitudinal direction, which is taken into account separately from the aforementioned stress fields. The stress in the ith tendon is limited by the condition:

$$\sigma_{pi} \leq f_{pd} \tag{4}$$

The resultants of axial and shear stress, plus the effect of the forces acting on the prestressing tendons, provide the resisting internal actions of the cross section, bending moment M_{Rd} and shear force V_{Rd} (while axial force N_{Rd} is null):

$$M_{Rd} = \int_S \sigma y dS + \sum_{n_p} A_{pi}y_{pi}\sigma_{pi}\cos\alpha_i = \sigma_{f1}\int_{S_{ft}} ydS + \sigma_{w1}\int_{S_{w1}} ydS + \sigma_{w2}\int_{S_{w2}} ydS + \sigma_{w3}\int_{S_{w3}} ydS + \sigma_{f2}\int_{S_{fb}} ydS + \sum_{n_p} A_{pi}y_{pi}\sigma_{pi}\cos\alpha_i \tag{5a}$$

$$V_{Rd} = \int_{S_{w3}} \tau dS + \sum_{n_p} A_{pi}\sigma_{pi}\sin\alpha_i = \tau b_w z_3 + \sum_{n_p} A_{pi}\sigma_{pi}\sin\alpha_i \tag{5b}$$

$$N_{Rd} = \int_S \sigma dS + \sum_{n_p} A_{pi}\sigma_{pi}\cos\alpha_i = \sigma_{f1}S_{ft} + \sigma_{w1}S_{w1} + \sigma_{w2}S_{w2} + \sigma_{w3}S_{w3} + \sigma_{fb}S_{f2} + \sum_{n_p} A_{pi}\sigma_{pi}\cos\alpha_i = 0 \tag{5c}$$

In the previous equations, the terms related to the areas S_{w1}, S_{w2}, and S_{w3} depend on the depth of the web layers z_1, z_2, and z_3, which may vary according to the following geometrical and static conditions:

$$z_1 \geq 0 \tag{6a}$$

$$z_2 \geq 0 \tag{6b}$$

$$z_1 + z_2 + z_3 = h_w \tag{6c}$$

$$z_3 \geq z_{3\min} \tag{6d}$$

In particular, Eq. (6d) states that the central web layer depth must be sufficient to bear shear stresses; its minimum value $z_{3\min}$,

which depends on concrete strength f_{cd2} and on transverse web reinforcement mechanical ratio ω_{wt}, is given by:

$$z_{3\min} = \frac{V_{Sd}}{f_{cd2} b_w \sqrt{\omega_{wt}(1-\omega_{wt})}} \quad \text{if } \omega_{wt} \leq 0.5 \tag{7a}$$

$$z_{3\min} = \frac{2V_{Sd}}{f_{cd2} b_w} \quad \text{if } \omega_{wt} > 0.5 \tag{7b}$$

It is obvious that the web depth h_w must be greater than $z_{3\min}$, otherwise shear equilibrium could not be satisfied.

Bending Moment–Shear Force Interaction Domains

The conditions of the previous section, managed according to nonlinear programming procedures, allow attainment of resistance domains of the cross section, for given web and flange reinforcements. Having defined the prestressing reinforcement ratio ρ_p and the longitudinal and transverse web reinforcement ratios ρ_{wl} and ρ_{wl}, the bending moment–shear force–flange reinforcement mechanical ratio (M_{Rd}–V_{Rd}–ρ_f interaction domains) may be determined according to the following steps:

1. Assign a pair of M_{Rd}, V_{Rd} values;
2. Evaluate the minimum web depth $z_{3\min}$ by Eq. (7); if $z_{3\min} > h_w$, it is not possible to proceed, because the whole web is not able to withstand shear stresses; a different M_{Rd}, V_{Rd} pair has to be considered;
3. Assign trial values of z_1, z_2, and z_3, satisfying Eq. (6);
4. Evaluate the shear stress τ by Eq. (5*b*);
5. Assign a trial value of angle ϑ in the range defined by Eqs. (3*b*) and (3*c*);
6. Assign trial values of σ_{w1}, σ_{w2}, and σ_{w3} in the ranges defined by Eqs. (2*a*), (2*b*), and (3*a*) respectively;
7. Assign trial values of σ_{pi}, satisfying condition (4);
8. Evaluate σ_{ft} and σ_{fb} by Eqs. (5*a*) and (5*c*);
9. Evaluate the longitudinal top and bottom flange reinforcement ratios ρ_{ft} and ρ_{fb} by Eq. (1) and the subsequent values of A_{ft} and A_{fb}; if necessary, increase them to fulfill other requirements, e.g., to obtain a given ratio of the longitudinal reinforcements of the top and bottom flange;
10. Repeat Steps 3 to 9, so as to minimize the total flange reinforcements, thus obtaining the value of ρ_f corresponding to the couple M_{Rd}, V_{Rd}; and
11. Repeat the whole procedure for different couples of M_{Rd}, V_{Rd} values, so as to obtain the whole M_{Rd}–V_{Rd}–ρ_f interaction domains.

More commonly, the interaction domains are plotted as normalized m–v–ω_f domains. These domains are a powerful and useful design tool both in the preliminary design, to accomplish the correct design of the cross section and, in the final control, to maximize the strength of the structural element. It is interesting to note that by imposing $A_p=0$, the procedure is applicable also to reinforced concrete beams.

In order to point out the performance of the method and to discuss the influence of bending moment–shear force interaction, a set of interaction domains for an I-shaped prestressed beam are presented here. The geometrical and mechanical characteristics of the concrete and steel components of the beam are shown in Fig. 3. Three-dimensional interaction domains obtained for $\omega_{wt}=0.3$

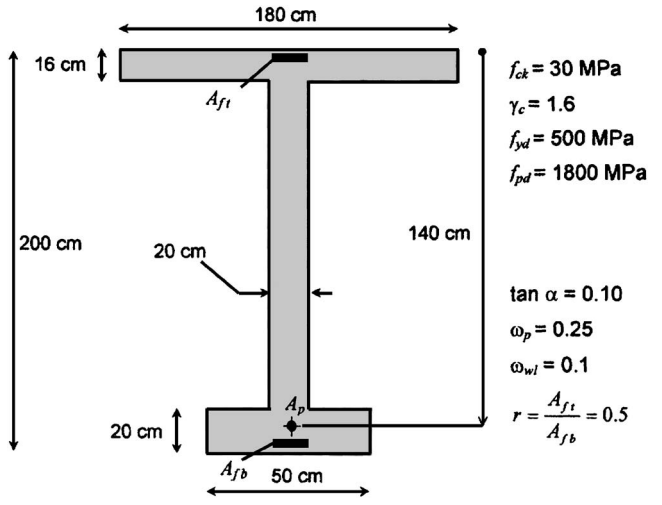

Fig. 3. I-shaped cross section of the bridge prestressed concrete beam

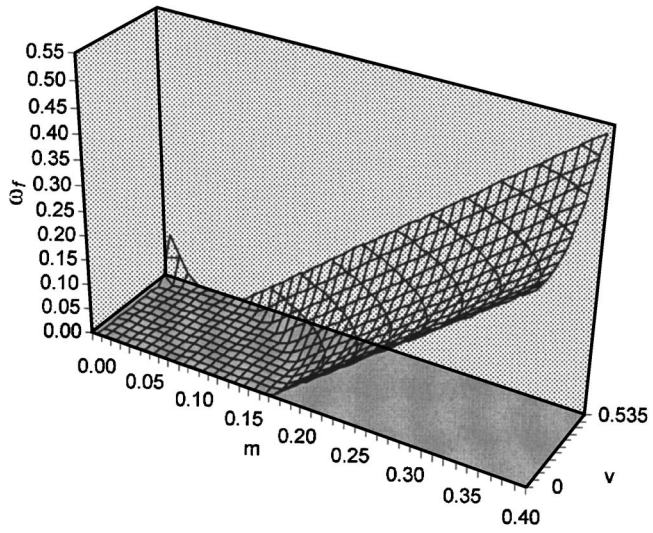

Fig. 4. m–v–ω_f interaction domain for $\omega_{wt}=0.3$

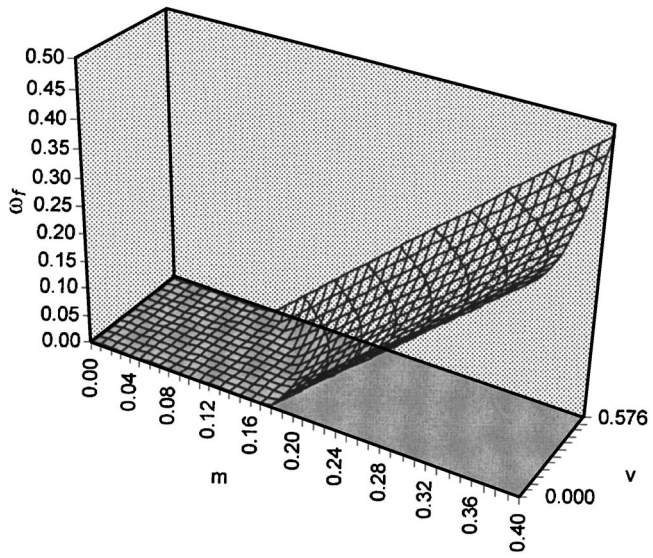

Fig. 5. m–v–ω_f interaction domain for $\omega_{wt}=0.5$

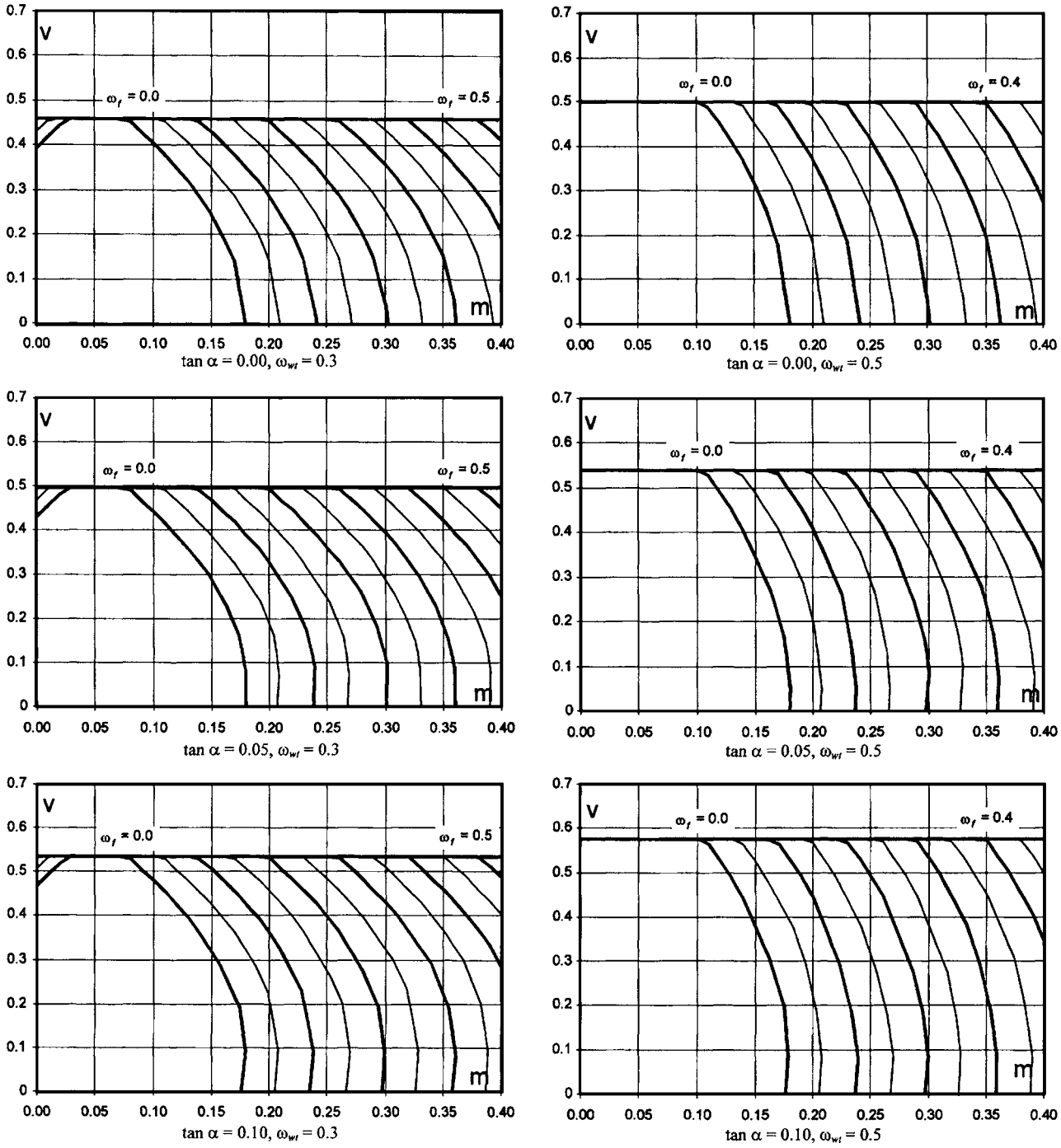

Fig. 6. m–v–ω_f interaction domains for tan α=0.00, 0.05, and 0.10, ω_{wf}=0.3 and 0.5

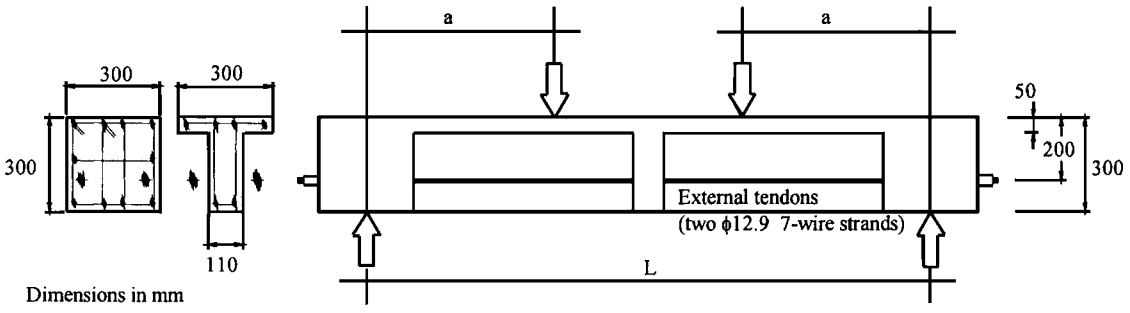

Fig. 7. T-shaped cross section and static scheme of the tested posttensioned beams

Table 1. Numerical over Experimental Ratios

	B_1	B_2
Beam 1[15]	0.695	0.775
Beam 2[15]	0.685	0.765
Beam 3[15]	0.620	0.690
Beam 4[15]	0.600	0.665
Beam 5[15]	0.650	0.720
Beam 6[15]	0.655	0.730
Beam 7[15]	0.720	0.800
Beam 8[15]	0.845	0.940
Beam 9[15]	0.650	0.725
BQ6[15]	0.695	0.810
BQ7[15]	0.680	0.795
BQ12[15]	0.605	0.605
BQ15[15]	0.720	0.850
BQ16[15]	0.605	0.605
BQ17[15]	0.605	0.680
BQ18[15]	0.615	0.715
BQ19[15]	0.665	0.780
ST-1[10]	0.800	0.810
ST-2[10]	0.845	0.855
ST-2C[10]	0.855	0.860
ST-2C+[10]	0.845	1.010
ST-2S[10]	0.655	0.670
ST-2P[10]	0.765	0.770
ST-3[10]	0.930	0.930
Mean value $\hat{\mu}$	0.709	0.773
$\hat{\sigma}$	0.097	0.102

and 0.5 are shown in Figs. 4 and 5 respectively; in both cases, the slope of the tendon is $\tan\alpha=0.10$.

Bidimensional interaction domains may be obtained as level curves of the limit surface in the m–v–ω_f space. Such diagrams are plotted in Fig. 6, for $\omega_{wt}=0.3$ and 0.5 and for $\tan\alpha=0$, 0.05, and 0.10. They clearly show that also in prestressed beams, there is a strong relation between bending moment and shear force, which cannot be neglected in design. The contribution of the prestressing tendons to the shear strength can also be observed in these figures. Higher shear strength is achieved with a higher inclination angle of the tendons (α) as observed by comparing the curves in the second and third rows ($\tan\alpha=0.05, \tan\alpha=0.10$) with those in the first row ($\tan\alpha=0.0$). It is finally evident that the increase in the transverse web reinforcement mechanical ratio ω_{wt} allows a reduction of the longitudinal flange reinforcement mechanical ratio ω_f. The domains thus give a clear view of the different possibilities in the arrangement of longitudinal transverse reinforcement in the cross section.

Comparison with Test Results

The reliability of the proposed model has been validated by comparing its numerical results to the strength values obtained by means of failure tests performed on thin-webbed prestressed concrete beams, reported in the literature (Tan and Ng 1998). The specimens, having a length ranging from 1,200 to 3,000 mm and a cross section depth of 300 mm, were externally prestressed by means of straight tendons (Fig. 7). Their T-shaped cross section was designed to fail in shear by crushing of the web concrete, after the stirrups yielded. Further details may be found in the original paper (Tan and Ng 1998).

The comparison has been carried on using a procedure already adopted by the writers in a previous paper (Recupero et al. 2003). In the proposed model, the concrete strength for uniaxial longitudinal stresses f_{cd1} have been evaluated neglecting the reduction coefficient 0.85 for long time actions and, for stresses in presence of transverse load f_{cd2}, the effectiveness shear factor is fixed as $0.70\cong0.60/0.85$ instead of 0.60 (because the tests were conducted in a short time), and the partial safety factor for concrete $\gamma_c=1$ (because the comparison is carried on with failure tests). Thus, it has been assumed

$$f_{cd1}=\left(1-\frac{f_{ck}}{250}\right)f_{ck}$$

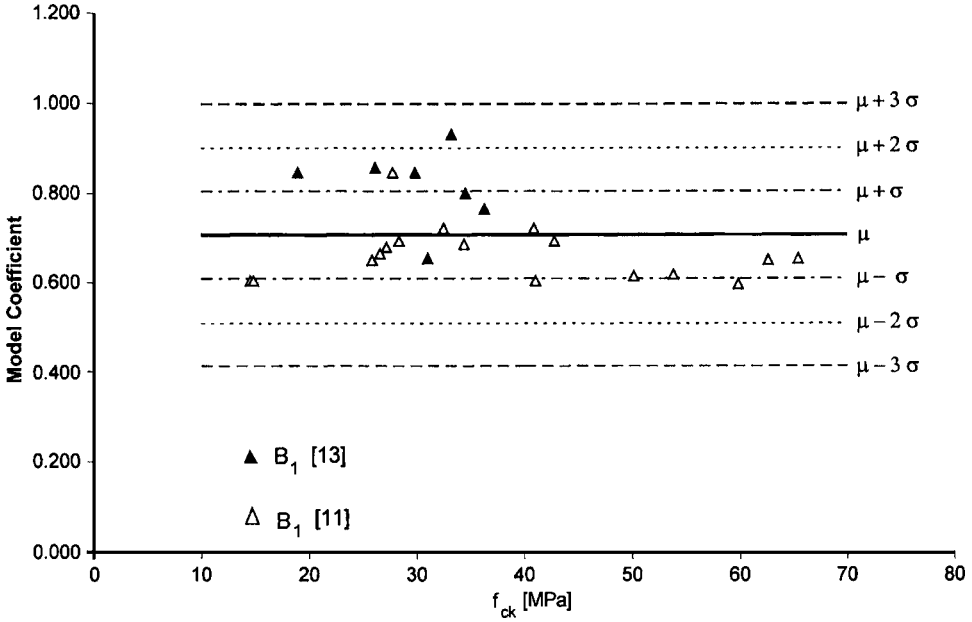

Fig. 8. Numerical over experimental values, plotted versus concrete strength for hypothesis B_1

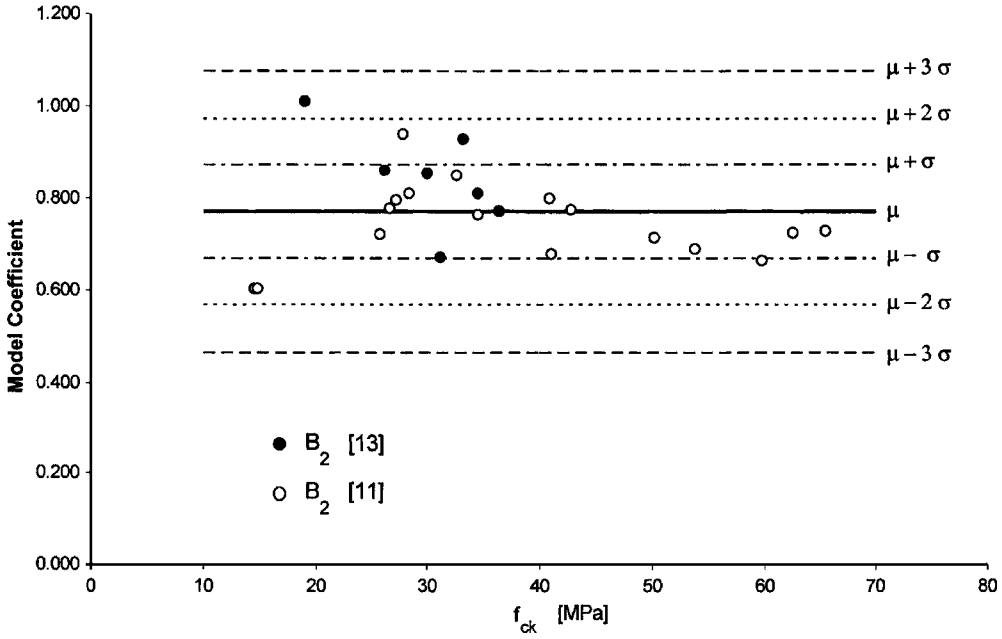

Fig. 9. Numerical over experimental values, plotted versus concrete strength for hypothesis B_2

$$f_{cd2} = 0.70\left(1 - \frac{f_{ck}}{250}\right) f_{ck}$$

In order to achieve better correlation with the experimental data, two different values for the depth of the web have been considered in the numerical model:

1. In the first case (B_1), it has been considered equal to the net depth of the web; and
2. In the second one (B_2), it has been assumed extended to the position of the longitudinal steel reinforcements of the bottom flange.

The ratios of the ultimate force values, numerically obtained by the proposed approach, over those given in the experiments are listed in Table 1. The table also includes the values for beams with ordinary longitudinal steel reinforcements (Recupero et al. 2003). The mean value $\hat{\mu}$ and the variance $\hat{\sigma}$ of these ratios give a probabilistic description of the results, assuming a Gaussian distribution and considering geometrical dimensions, loads and mechanical characteristics as deterministic values.

In Figs. 8 and 9, the ratios of numerical over experimental strength are plotted versus the concrete strength together with lines defining the mean value, plus 1,2,3 times the variance, up to the characteristic value $\hat{\mu}+3\hat{\sigma}$. The results show that the numerical model gives a lower bound solution and confirm its adequate reliability for all the values of concrete strength.

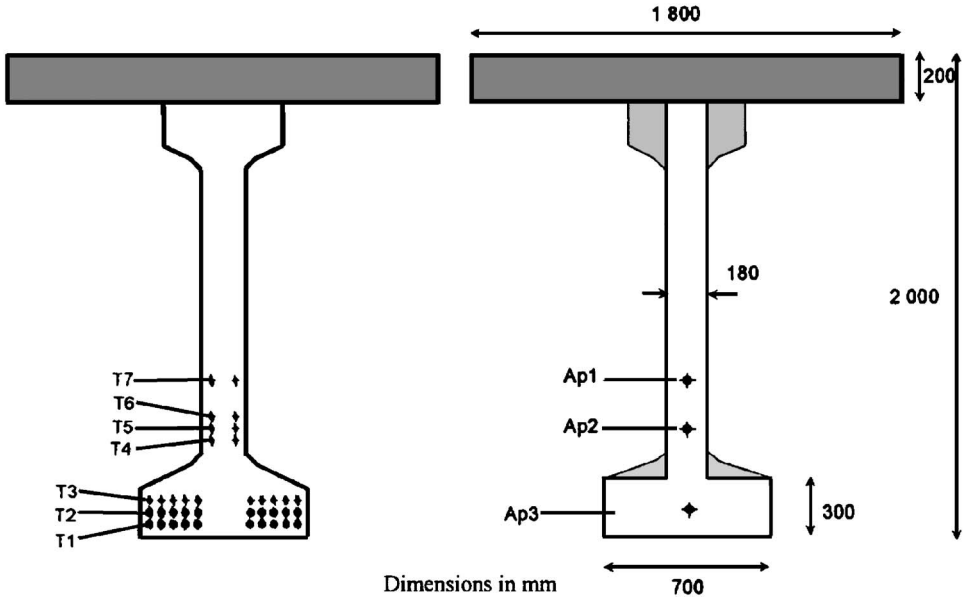

Fig. 10. Actual cross section of the beam and simplified model used in the design

Table 2. Number, Position, Type, and Area of the Prestressing Steel Tendons

Strand	Number	Distance from the bottom (mm)	Type (in.)	Area (mm^2)	Prestressing level (MPa)	Debonding from the beam ends (mm)
T1	2	50	0.6	139	1,419	850
T1	2	50	0.6	139	1,419	500
T1	2	50	0.6	139	1,419	400
T1	4	50	0.6	139	1,419	200
T2	2	100	0.6	139	1,419	500
T2	2	100	0.6	139	1,419	300
T2	4	100	0.6	139	1,419	200
T2	2	100	0.6	139	1,419	200
T3	10	150	0.6	139	1,419	—
T4	2	400	0.6	139	1,419	—
T5	2	450	0.6	139	1,419	—
T6	2	500	0.6	139	1,419	—
T7	2	650	0.6	139	1,419	—

Design Procedure for a Bridge Prestressed Concrete Beam

Aiming at illustrating the effectiveness of the proposed approach, it has been used in the design of a pretensioned bridge beam. Such a typology has been selected because two reasons make it particularly sensitive to the M–V interaction: The use of bare strands, without any duct, allows a reduction of web width, with subsequent increase of shear stresses; the straightness of the steel cables does not allow the reduction of the effective shear force, usually provided by curvilinear posttensioned tendons.

Fig. 10 shows the cross section of the beam and the simplified model used in the analysis. The number, distance from the bottom, area, and debonding of the strands are described in Table 2. The characteristic values of the compressive strength of the concrete are f_{ck}=30 MPa for the slab and f_{ck}=40 MPa for the beam. The yield strength of the ordinary reinforcement and of the prestressing steel are f_{yk}=430 MPa and f_{pk}=1670 MPa, respectively. The design values of the strength have been calculated assuming partial safety factors γ_c=1.6 and γ_s=1.15. The design was performed by subdividing the beam in portions with a length shorter than the depth. A longitudinal elevation of the beam and the location of the reference points used in the analysis are shown in Fig. 11. Tables 3 and 4 report the values of internal actions in the design sections and the transverse web reinforcement assumed in each section, respectively.

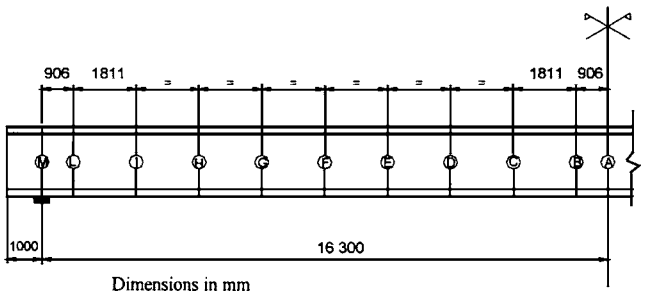

Fig. 11. Static scheme of the pretensioned concrete beam

Table 3. Internal Actions at Assigned Sections

Section	x (m)	V_{Sd} (kN)	M_{Sd} (kNm)
M	1.00	1,433.3	-44.0
L	1.91	1,353.6	1,217.9
I	3.72	1,194.4	3,525.3
H	5.53	1,035.1	5,544.2
G	7.34	875.9	7,274.7
F	10.15	716.6	8,716.8
E	10.96	557.4	9,870.5
D	12.77	398.1	10,735.8
C	14.58	238.9	11,312.6
B	16.39	79.6	11,601.0
A	17.30	0.0	11,637.1

The proposed procedure was used for evaluating the additional longitudinal reinforcement necessary in each section, after having assumed a tentative value of the longitudinal web reinforcement. In order to point out the relation between flange and web longitudinal reinforcement, five values of the latter have been used, starting from a null value (although this is only a theoretical possibility, because a flange longitudinal reinforcement shall always be used) up to 10ϕ12. The longitudinal flange reinforcements necessary, evaluated assuming r=1, i.e., A_{ft}=A_{fb}, are shown in Table 5.

It is evident that the longitudinal steel demand in the flanges decreases as the web longitudinal reinforcement increases. Additional reinforcement is necessary at the ends, where the shear force reaches the maximum.

Conclusions

This paper extends a model previously proposed for the evaluation of M–N–V interaction of the box and I-shaped reinforced concrete cross sections of structural elements to prestressed concrete elements. The M–V domains thus obtained point out the mutual influence of bending moment and shear force and its dependence on the value of transverse web reinforcement.

The comparison of the results given by the proposed approach to the strength provided by tests described in the literature confirms that the numerical model gives a lower bound solution. The model is particularly reliable when different concrete strengths,

Table 4. Transverse Web Reinforcement

Section	x (m)	Diameter (mm)	Spacing (mm)
M	1.00	ϕ 10	100
L	1.91	ϕ 10	125
I	3.72	ϕ 10	150
H	5.53	ϕ 10	150
G	7.34	ϕ 10	200
F	10.15	ϕ 8	200
E	10.96	ϕ 8	200
D	12.77	ϕ 8	200
C	14.58	ϕ 6	200
B	16.39	ϕ 6	200
A	17.30	ϕ 6	200

Table 5. Longitudinal Reinforcement in Flanges

Section	Longitudinal web reinforcement (mm^2)				
	0	10ϕ6	10ϕ8	10ϕ10	10ϕ12
M	2,496	2,320	2,206	2,062	1,891
L	906	762	649	505	334
I	0	0	0	0	0
H	0	0	0	0	0
G	0	0	0	0	0
F	0	0	0	0	0
E	0	0	0	0	0
D	0	0	0	0	0
C	0	0	0	0	0
B	0	0	0	0	0
A	0	0	0	0	0

f_{cd1} for uniaxial longitudinal stresses and f_{cd2} for stresses in presence of transverse load, are used together with the assumption that the web is extended to the position of the longitudinal steel reinforcements of the bottom flange. Its validity for reinforced concrete members, as previously demonstrated, allow us to conclude that the proposed model is able to describe in an accurate way, with a unified approach, both reinforced concrete and prestressed concrete elements.

Notation

The following symbols are used in this paper:

A_{fj} = longitudinal reinforcement in flanges (j=t,b, with t=top and b=bottom);
$A_p=\Sigma_{n_p}A_{pi}$ = total area of the tendons;
A_{pi} = area of the ith tendon;
A_{wl} = longitudinal web reinforcement;
A_{wt} = transverse web reinforcement;
b_w = web width;
$f_{cd1}=0.85(1-f_{ck}/250)(f_{ck}/\gamma_c)$ = design strength of concrete, for long period uniaxial load (f_{ck} in MPa);
$f_{cd2}=0.60(1-f_{ck}/250)(f_{ck}/\gamma_c)$ = design strength of concrete, in presence of transverse load (f_{ck} in MPa);
f_{ck} = characteristic strength of concrete;
f_{pd} = design strength of steel prestressing tendons;
f_{yd} = design yield strength of ordinary steel reinforcement;
H = depth of the whole cross section;
h_w = web depth;
$m=M/SHf_{cd1}$ = normalized bending moment;
M_{Rd} = resisting bending moment;
M_{Sd} = design bending moment;
N_{Rd} = resisting axial force;
n_p = number of prestressing tendons;
$r=A_{ft}/A_{fb}$ = geometrical ratio of longitudinal flange reinforcements (t=top, b=bottom);
S = area of the whole cross section;
S_{fj} = area of top or bottom flange (j=t,b, with t=top and b=bottom);
S_{wi} = area of web layers (i=1,2,3);
s = spacing of transverse web reinforcement;
V_{Rd} = resisting shear force;
V_{Sd} = design shear force;
$\nu=V/b_wh_wf_{cd2}$ = normalized shear force;
y_{pi} = position of the ith tendon;
z_i = depth of the web layers (i=1,2,3);
$z_{3\min}$ = minimum depth of the central web layer;
α_i = angle of the ith tendon on the longitudinal direction;
γ_c = partial safety factor for concrete;
γ_s = partial safety factor for steel;
ϑ = angle of compressive stress field on the longitudinal direction;
$\rho_{fj}=A_{fj}/S_{fj}$ = longitudinal flange reinforcement ratio (j=t,b, with t=top and b=bottom);
$\rho_p=A_p/S$ = prestressing reinforcement ratio;
$\rho_{wl}=A_{wl}/b_wh_w$ = longitudinal web reinforcement ratio;
$\rho_{wt}=A_{wt}/b_ws$ = transverse web reinforcement ratio;
σ_{fj} = axial stress in flange layers (j=t,b, with t=top and b=bottom);
σ_{pi} = axial stress in the ith tendon;
σ_{wi} = axial stress in web layers (i=1,2,3);
τ = shear stress in the central web layer;
$\omega_f=(A_{ft}+A_{fb}/S)(f_{yd}/f_{cd1})$ = total longitudinal flange reinforcement mechanical ratio;
$\omega_p=(A_p/S)(f_{pd}/f_{cd1})$ = prestressing reinforcement mechanical ratio;
$\omega_{wl}=(A_{wl}/b_wh_w)(f_{yd}/f_{cd2})$ = longitudinal web reinforcement mechanical ratio; and
$\omega_{wt}=(A_{wt}/b_wS)(f_{yd}/f_{cd2})$ = transverse web reinforcement mechanical ratio.

References

ACI Committee 318. (1983). "Building code requirements for reinforced concrete (ACI 318-95) and commentary ACI 318 R-95." American Concrete Institute, Detroit.

Bach, F., Nielsen, M. P., and Braestrup, M. W. (1978). "Rational analysis of shear in reinforced concrete beams." *IABSE Proc.*, P-15/78, 1–16.

Comittè Eurointernational du Bèton (CEB-FIP). (1993). "Model code for concrete structures for buildings." CEB, Lausanne.

Collins, M. P., Mitchell, D., Adebar, P., and Vecchio, F. J. (1996). "A general shear design method." *ACI Struct. J.*, 93(1), 36–45.

EC2. (1996). "Design of concrete structures—Part. 1: General rules for buildings," CEN, Brussels.

Fanti, G., and Mancini, G. (1994). "Shear-prestressing interaction in ultimate limit state design." *Proc., Developments in Short and Medium Span Bridge Engineering*, Halifax, Canada.

Fanti, G., Mancini, G., and Recupero, A. (1995). "Shear and torsion design of structures prestressed with unbonded tendons." *General C.E.B. Assembly*, Berlin.

Fanti, G., and Mancini, G. (1995). "Shear, normal force, bending moment interaction in bridge piers." *Proc., 1st Japan–Italy Workshop on Seismic Design and Retrofit of Bridges*, Tsukuba, Japan.617–628.

Haddadin, M. J., Hong, S. T., and Mattock, A. H. (1971). "Stirrup effectiveness in reinforced concrete beams with axial force." *J. Struct. Div. ASCE*, 97(9), 2277–2297.

Mancini, G., and Recupero, A. (2000). "Interaction of axial force, bend-

ing moment, and shear force in RC structures" ("Interazione tra Azione assiale, Momento e Taglio nelle Strutture in c.a."). *Studi e Ricerche, Scuola di Specializzazione in Costruzioni in C.A.*, Fratelli Pesenti, Politecnico di Milano, Vol. 20, 127–146 (in Italian)

Mattock, A. H. (1969). "Diagonal tension cracking in concrete beams with axial force." *J. Struct. Div. ASCE*, 95(9), 1887–1990.

Puleri, G., and Russo, G. (1997). "Stirrup effectiveness in reinforced concrete beams under flexure and shear." *ACI Struct. J.*, 94(3), 227–238.

Puleri, G., Russo, G., and Zingone, G. (1991). "Flexure-shear interaction model for longitudinally reinforced beams." *ACI Struct. J.*, 88(1), 60–68.

Recupero, A., D'Aveni, A., and Ghersi, A. (2003). "*N–M–V* interaction domains for box and I-shaped reinforced concrete members." *ACI Struct. J.*, 100(1), 113–119.

Schlaich, J., Shäfer, K., and Jennwein, M. (1987). "Toward a consistent design of structural concrete." *PCI J.* 32(3)74–150.

Tan, K.-H. and Ng, C.-K. (1998). "Effect of shear in externally prestressed beams." *ACI Struct. J.*, 95(2), 116–128.